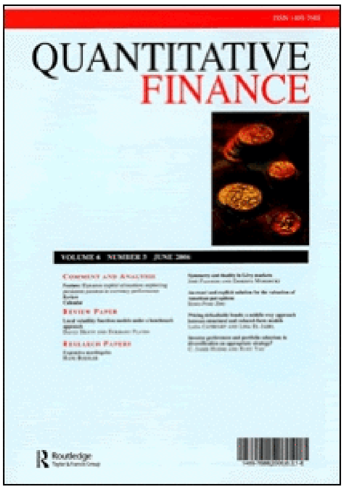

Quantitative Finance
Publication details, including instructions for authors and subscription information:
http://www.informaworld.com/smpp/title~content=t713665537

On the valuation of fader and discrete barrier options in Heston's stochastic volatility model

Susanne A. Griebsch[a]; Uwe Wystup[b]
[a] School of Finance and Economics, University of Technology, Broadway, NSW 2007, Australia [b] Center for Practical Quantitative Finance, Frankfurt School of Finance & Management, 60314 Frankfurt am Main, Germany

First published on: 13 December 2010

Quantitative Finance, 2010, 1–17, iFirst

Routledge
Taylor & Francis Group

On the valuation of fader and discrete barrier options in Heston's stochastic volatility model

SUSANNE A. GRIEBSCH*† and UWE WYSTUP‡

†School of Finance and Economics, University of Technology, Sydney, PO Box 123, Broadway, NSW 2007, Australia
‡Center for Practical Quantitative Finance, Frankfurt School of Finance & Management, Sonnemannstrasse 9–11, 60314 Frankfurt am Main, Germany

(*Received 4 February 2009; in final form 17 June 2010*)

We focus on closed-form option pricing in Heston's stochastic volatility model, where closed-form formulas exist only for a few option types. Most of these closed-form solutions are constructed from characteristic functions. We follow this closed-form approach and derive multivariate characteristic functions depending on at least two spot values for different points in time. The derived characteristic functions are used as building blocks to set up (semi-) analytical pricing formulas for exotic options with payoffs depending on finitely many spot values such as fader options and discretely monitored barrier options. We compare our result with different numerical methods and examine the computational accuracy.

Keywords: Exotic options; Heston model; Characteristic function; Multidimensional FFT

1. Introduction to the Heston model

The stochastic volatility model of Heston is characterized by the following system of stochastic differential equations:

$$\begin{aligned} \frac{\mathrm{d}S_t}{S_t} &= r\mathrm{d}t + \sqrt{v_t}\mathrm{d}W_t^S, \\ \mathrm{d}v_t &= \kappa(\theta - v_t)\mathrm{d}t + \sigma\sqrt{v_t}\,\mathrm{d}W_t^v, \end{aligned} \tag{1}$$

with

$$\mathrm{d}W_t^S \mathrm{d}W_t^v = \rho\,\mathrm{d}t.$$

The processes $\{S_t\}_{t\geq 0}$ and $\{v_t\}_{t\geq 0}$ denote the spot price and instantaneous variance, respectively. The variance process $\{v_t\}$ is driven by a mean-reverting stochastic square-root process. The two Wiener processes $\{W^S\}$ and $\{W^v\}$ are correlated with the correlation rate ρ. In a Foreign Exchange (FX)§ setting the risk-neutral drift term r of the underlying price process is set to the difference between the domestic and foreign interest rates $r_\mathrm{d} - r_\mathrm{f}$.

All five parameters of the Heston model, i.e. the long-term variance θ, the rate of mean reversion κ, the volatility of variance σ, the correlation ρ and the initial variance v_0, are assumed to be constant and satisfy

$$\theta > 0, \quad \kappa > 0, \quad \sigma > 0, \quad |\rho| < 1, \quad v_0 \geq 0. \tag{2}$$

The term $\sqrt{v_t}$ in equation (1) ensures the use of non-negative volatility in the spot price process in a continuous theory. It is well known that the distribution of values of the variance process is given by a non-central chi-squared distribution. This distribution is defined on the non-negative real line and, hence, the probability that the variance takes a negative value is equal to zero. According to Feller's classification of the boundary points, the process $\{v_t\}_{t\geq 0}$ can never reach infinity. Moreover, if $v_0 > 0$ and $2\kappa\theta/\sigma^2 > 1$, the process $\{v_t\}_{t\geq 0}$ is always positive (for example, see Lipton 2001, p. 235).

Stochastic volatility models are useful because they explain the 'volatility smile', the empirical phenomenon that options with different moneyness and expirations

*Corresponding author. Email: susanne.griebsch@uts.edu.au
§The role of the Heston model in Foreign Exchange Options is very dominant. FX Options business is heavily driven by stochastic volatility models. There are two models essentially used in practice: The Heston model for pricing exotic options and the SABR model to build the FX volatility smile. We find the Heston model in many software products used in the market, including Bloomberg, LPA and most in-house production software of investment banks.

Quantitative Finance
ISSN 1469–7688 print/ISSN 1469–7696 online © 2010 Taylor & Francis
http://www.informaworld.com
DOI: 10.1080/14697688.2010.503375

have different Black–Scholes implied volatilities. More interestingly, the values of exotic options given by models based on Black–Scholes assumptions can deviate significantly from market prices and option traders are motivated to find models that can take the volatility smile into account. Therefore, pricing methods for exotic options in stochastic volatility models need to be developed. This study contributes to these methods by concentrating on the development of a benchmark method that might be of assistance to validate numerical or other approximation methods for the valuation of weakly path-dependent options.

1.1. Option pricing in the Heston model

In the Black–Scholes model, there is only one source of randomness in the spot price process and contingent claims can be hedged by trading in the money market and the underlying security itself. In the Heston model case, random changes in volatility also need to be hedged in order to form a self-financing hedge portfolio and therefore to price contingent claims by the no-arbitrage principle. Thus, to achieve this kind of model 'completeness' (in the sense that every contingent claim can be replicated by a self-financing trading strategy in the underlying securities) in the Heston model, we assume that in addition to trading in the money market and the underlying security, we can trade in another liquid security, which depends on time, volatility and the underlying spot price process. With these three basic securities, we can set up a self-financing hedge portfolio that replicates a general contingent claim with value function $V(t, v, S)$.

As shown by Hakala and Wystup (2002) in a Foreign Exchange setting, the value function V satisfies

$$0 = V_t + (\kappa\theta - \kappa + \lambda)v)V_v + (r_{\mathrm{d}} - r_{\mathrm{f}})SV_S + \frac{1}{2}\sigma^2 vV_{vv} + \frac{1}{2}vS^2V_{SS} + \rho\sigma vSV_{vS} - r_{\mathrm{d}}V$$

in the region $0 \le t \le T$, $0 < S < \infty$ and $0 \le v < \infty$. The variable λ is used to denote the market price of volatility risk, which is set to zero in this paper without loss of generality. A solution to the above equation can be obtained by specifying appropriate exercise and boundary conditions, which depend on the contract specification.

1.2. Numerical pricing methods versus (semi-) analytical pricing formulas

In stochastic volatility models in general, options can be priced using analytical formulas or numerical methods. Numerical pricing of exotic options in the Heston model can be carried out using conventional numerical methods such as Monte Carlo simulation, finite differences, tree methods or an exact simulation method. Monte Carlo simulation in the Heston model has been explored, for example, by Higham and Mao (2005), Andersen (2008) and Lord *et al.* (2009). An introduction to finite difference methods in the Heston model is given by Kluge (2003). A method to simulate logarithmic spot values with respect to its exact probability distribution was developed by Broadie and Kaya (2006). When evaluating exotic options with numerical methods, one faces two difficulties. First, depending on which exotic option to price, choosing the adequate numerical method, and, second, once the method is selected, how to deal with the challenges of the numerical method itself.

Monte Carlo simulation, for instance, is a robust and strong method that can be used for pricing almost every (especially path-dependent) option. But in the Heston model, one aspect has to be taken into account, if Monte Carlo is the numerical method of choice: The use of Monte Carlo methods in the Heston model depends on the choice of the model parameters κ, θ, σ and v_0. Discretization of the variance process with a Euler scheme, for example with times u and t, $u<t$, leads to

$$v_t = v_u + \kappa(\theta - v_u)(t-u) + \sigma\sqrt{v_u}z\sqrt{t-u}, \quad z \sim \mathcal{N}(0,1).$$

It follows, that by discretizing this process we modify the probability of obtaining a negative value for the variance. As Lord *et al.* (2009) point out, by using Euler discretization we change it from zero to something normally distributed and therefore positive with probability

$$\mathbb{P}(v_t < 0) = N\left(\frac{-v_u - \kappa(\theta - v_u)(t-u)}{\sigma\sqrt{v_u(t-u)}}\right).$$

Higham and Mao (2005) and Lord *et al.* (2009) deal with this problem by setting up various first- and second-order discretization schemes for the volatility process and by investigating convergence and approximation aspects of the resulting vanilla and barrier option prices. One possible solution to this problem would be to find a discretization scheme that does not change the probability of negative variance values and still maintains the speed of simulating with a Euler scheme.

Hence, although a number of efficient numerical methods to compute option values is available, it is advantageous to have analytical solutions for the value of a financial instrument within a given model, as the solutions obtained will be exact and can be used as a benchmark. Furthermore, the available methods to compute them work independent of the model, contrary to numerical simulation methods. For example, the use of Monte Carlo methods in the Heston model for the variance process is critical because of the Lipschitz continuity condition. Numerical methods to approximate integrals such as in (3), just like numerical integration or fast Fourier transforms, can be used in full generality across a number of different models, since they are techniques that are employed and explored in a wide field of applications. Applying these methods, we can benefit from the research advances made in this area and from the important fact that they are not dependent on the choice of the parameter set in the Heston model—Feller's stability condition† $2\kappa\theta/\sigma^2 > 1$ is no longer a constraint on the model parameters.

Closed-form option valuation in the Heston model has so far been limited to a few option types. Heston provided a closed-form solution for European vanilla options in his original paper (Heston 1993). The call value at time $t < T$ with maturity T and strike price K is given by

$$\text{Call} = \mathrm{e}^{-r_\mathrm{f}(T-t)} S_t P_S - K\mathrm{e}^{-r_\mathrm{d}(T-t)} P_N, \tag{3}$$

where, for $j = N, S$,

$$P_j = \frac{1}{2} + \frac{1}{\pi}\int_0^\infty \Re\left[\frac{\exp(-iu\ln K)\varphi_j(u)}{iu}\right]\mathrm{d}u. \tag{4}$$

The function $\varphi_j(u) = \exp(B_j(u) + A_j(u)v_t + iu\ln S_t)$ denotes the characteristic function of the random variable $\ln S_T$ at time t under two different measures $(j = N, S)$. The functions A and B depend on the time to maturity $T - t$, interest rates r_d and r_f and the set of constant model parameters κ, ρ, θ and σ. Mikhailov and Nögel (2003) derived the one-dimensional characteristic function for the case of piecewise constant parameters using an iterative approach to solve the Ricatti equations by means of adjusting their initial conditions. Lord (2006) derived pricing techniques using transform techniques for one-dimensional affine models in the context of evaluating lower bounds for Asian options.

Other closed-form solutions for various types of options in the Heston model have been reported by a number of researchers.

- Grünbichler and Longstaff (1996): *Volatility Option*. The transition density of the volatility process is known to be a non-central chi-squared distribution.
- Dempster and Hong (2000): *Correlation Option*. The characteristic function of two spot prices at maturity is derived in a two-factor model with stochastic volatility.
- Zhu (2000): *Exchange, Chooser and Product Option, Barrier Option on Futures for* $\rho = 0$. Formulas for the above options are derived via the characteristic functions of $\ln S_T$.
- Faulhaber (2002): *Double Barrier Option for* $\rho = 0$ *and* $r_\mathrm{d} = r_\mathrm{f}$. Two methods are presented to derive analytical solutions for this special class of path-dependent options: the method of images and the eigenfunction expansion approach. It was shown that a generalization for Heston's model without the above restrictions ($\rho = 0$ and $r_\mathrm{d} = r_\mathrm{f}$) fails for both methods.
- Kruse and Nögel (2005): *Forward Start Option*. The derivation is based on the fact that, at the determination time of the strike, the option price probabilities are not dependent on the actual spot price. Therefore, the formulas are derived by solving expectations via the transition density of v.
- Chiarella and Ziogas (2009): *American Option*. The pricing problem is formulated as the solution to an inhomogeneous partial differential equation. The corresponding homogeneous problem is solved using Laplace and Fourier transforms and this solution is extended to the solution to the inhomogeneous case with the application of Duhamel's principle. An integral equation is provided for the early exercise region of the option.

Summing up, we may state that, so far, closed-form formulas in the Heston model mostly exist for options that are dependent on one spot value at maturity, $\ln S_T$, on values of the volatility at intermediate dates, $v_{t_1}, \ldots, v_{t_n}$, or are only valid in a reduced Heston model framework with uncorrelated Brownian motions, $\rho = 0$. The recent results for the forward start and American option provide formulas for options with a payoff dependent on the path of the spot price and are in line with this work. We extend the above list of applications of option valuation under the Heston's stochastic volatility dynamics to include weakly path-dependent products.

1.3. *Results of this paper and Outline*

With Heston's formula (3) and the formulas of Zhu (2000) we can identify a general format of a certain type of closed-form solution in the Heston model. These solutions are essentially based on probabilities such as $\mathbb{P}(S > c)$, where c is a constant and S some random spot value. These probabilities can be expressed in terms of distribution functions $F(c)$, which in turn can be determined by evaluating Fourier integrals with respect to characteristic functions, as in the case of call options in (4). We make use of this observation to establish (semi-)analytical formulas for exotic options with a payoff function, which depends on finitely many spot price values at fixed times $0 < t_1 < \cdots < t_n$ in the following respect:

$$\text{Payoff}(S_{t_1}, \ldots, S_{t_n}) = (\pm(S_{t_n} - K))^+ \times f(\mathbb{1}_{\{S_{t_i} \lessgtr b_i\}} \mathbb{1}_{\{v_{t_i} \lessgtr b_i\}}). \tag{5}$$

The function f defines a combination of indicators $\mathbb{1}_{\{S_{t_i} \leq b_i\}}$, $\mathbb{1}_{\{S_{t_i} \geq b_i\}}$, $\mathbb{1}_{\{v_{t_i} \geq c_i\}}$ or $\mathbb{1}_{\{v_{t_i} \leq c_i\}}$ $(i = 1, \ldots, n)$ with respect to the operations $-$, $\times$ and $+$, and the boundaries b_i and c_i are deterministic. Fader options and discrete barrier options are indicative examples of such combinations. Therefore, we derive multivariate characteristic functions that allow us to compute values of options of type (5) in closed form.

The remainder of the paper is organized as follows: In section 2 we derive multivariate characteristic functions

†If $2\kappa\theta/\sigma^2 < 1$, assuming that $v_0 > 0$, the origin is accessible and strongly reflecting. That is why in this situation the probability of hitting zero is quite significant and the process v often has a strong affinity for the area around the origin (Andersen 2008). Simulating this process at discrete time points therefore frequently leads to the problem of generating negative volatility values and therefore many sources suggest including the Feller condition as a constraint in the model calibration to market data.

dependent on random future values of the logarithmic spot. This result plays a central role throughout this paper, since its existence in closed form enables us to apply it to the valuation of exotic options, in particular fader options and discrete barrier options. These options are discussed in sections 3 and 4. We consider the general problem of evaluating these claims through a model-independent formula (with respect to an equivalent martingale measure) and apply the results derived in the previous sections to obtain solutions for the valuation problem in the Heston model. In section 5 we discuss the calculation of the probabilities contained in the established analytical formulas and present numerical examples.

2. Characteristic functions

In this section, we derive n-variate characteristic functions of the logarithmic spot prices $\ln S_{t_1}, \dots, \ln S_{t_n}$ at times $0 < t_1 < \cdots < t_n = T$ in the Heston model under two different probability measures. This result is used to establish closed-form valuation formulas for various exotic options in sections 3 and 4.

2.1. Derivation of the n-variate characteristic function

Let $X = (X_1, \dots, X_n)'$ be a random vector and $u = (u_1, \dots, u_n)$ be a vector of real numbers. The joint characteristic function of n random variables $X_1, \dots, X_n$ is defined by

$$\varphi_X(u) = \mathbb{E}[e^{iuX}] = \int_{\mathbb{R}^n} \exp(iu_1x_1 + \cdots + iu_nx_n)\mathrm{d}\mathbb{P}^X,$$

where $\mathbb{P}^X$ is the probability measure function of X. If not denoted otherwise, we understand the expectation value to be under the trivial σ-field $\mathcal{F}_{t_0}$. The function $\varphi_X(u)$ is a complex-valued continuous function of the n real variables $u_1, \dots, u_n$. We derive the characteristic function under the risk-neutral measure $\mathbb{Q}_N$ and the S-measure $\mathbb{Q}_S$ with the spot price as numeraire.

Theorem 2.1: *In the Heston model as defined in* (1) *the joint characteristic function of the logarithm of spot values* $X = (x_{t_1}, \dots, x_{t_n})$ *at times* $0 = t_0 < t_1 < \cdots < t_n = T$ *under the risk-neutral measure* $\mathbb{Q}_N$ *is given by*

$$\varphi_X^N(u_1, \dots, u_n) = \exp\left(\sum_{k=1}^n iu_kh(t_k) - \sum_{k=1}^n q(u_k)j(t_k) + \sum_{k=1}^n B_k + A_nv_0\right), \tag{6}$$

where we set

$$B_k = B\left(t_{n-k+1} - t_{n-k}, q(u_{n-k+1}) + A_{k-1}, p\left(\sum_{j=n-k+1}^n u_j\right)\right), \tag{7}$$

$$A_k = A\left(t_{n-k+1} - t_{n-k}, q(u_{n-k+1}) + A_{k-1}, p\left(\sum_{j=n-k+1}^n u_j\right)\right), \tag{8}$$

starting with $A_0 = 0$ *and*

$$h(t) = x_0 + (r_\mathrm{d} - r_\mathrm{f})t, \tag{9}$$

$$j(t) = v_0 + \kappa\theta t. \tag{10}$$

The functions A and B are defined as

$$A(\tau) = A(\tau, a, b) = \frac{da(1 + \mathrm{e}^{-\mathrm{d}\tau}) - (1 - \mathrm{e}^{-d\tau})(2b + \kappa a)}{\gamma}, \tag{11}$$

$$B(\tau) = B(\tau, a, b) = \frac{\kappa\theta}{\sigma^2}(\kappa - d)\tau + \frac{2\kappa\theta}{\sigma^2}\ln\frac{2d}{\gamma}, \tag{12}$$

with

$$d = \sqrt{\kappa^2 + 2\sigma^2 b},$$
$$\gamma = d(1 + \mathrm{e}^{-\mathrm{d}\tau}) + (\kappa - \sigma^2 a)(1 - \mathrm{e}^{-\mathrm{d}\tau}),$$

and the functions p and q as

$$p(u) = \left(\frac{1}{2} - \kappa\frac{\rho}{\sigma} - \frac{1}{2}iu(1 - \rho^2)\right)iu, \tag{13}$$

$$q(u) = iu\frac{\rho}{\sigma}. \tag{14}$$

The n-variate characteristic function under the S-measure $\mathbb{Q}_S$ *is given by*

$$\varphi_X^S(u_1, \dots, u_n) = \exp\left(\sum_{k=1}^n iu_kh(t_k) - \sum_{k=1}^n q(u_k)j(t_k) - \frac{\rho}{\sigma}j(t_n) + \sum_{k=1}^n B_k + A_nv_0\right), \tag{15}$$

with a different definition of the functions A and B than for φ^N, *namely*

$$B_k = B\left(t_{n-k+1} - t_{n-k}, q(u_{n-k+1}) + A_{k-1}, p\left(\sum_{j=n-k+1}^n u_j - i\right)\right),$$
$$A_k = A\left(t_{n-k+1} - t_{n-k}, q(u_{n-k+1}) + A_{k-1}, p\left(\sum_{j=n-k+1}^n u_j - i\right)\right),$$

starting with $A_0 = \rho/\sigma$.

Remark 1: Note that the exponents of the exponential function in φ^N and φ^S are linearly dependent on the state variables at time 0, v_0 and x_0. The functions A and B are defined recursively. Both functions call as an argument the value of A in the previous step. For $n = 1$ the result in theorem 2.1 reduces to the univariate characteristic function that is used in the closed-form formula for vanilla options by Heston.

Proof: The goal is to derive the characteristic function for two different measures, the risk-neutral $\mathbb{Q}_N$ and the S-measure $\mathbb{Q}_S$ with S as its numeraire.

For $n=1$ the characteristic functions are known. We use induction, beginning with the characteristic function of two random logarithmic spot values at two different points in time t_1 and t_2 with $0<t_1<t_2$. Let x_t denote the logarithmic spot value $\ln S_t$ at an arbitrary time $0<t\le t_2$. Then we denote the Radon–Nikodym derivatives corresponding to the measures $\mathbb{Q}_N$ and $\mathbb{Q}_S$ by

$$g_N(t_2)=1, \quad g_S(t_2)=\exp(-(r_\mathrm{d}-r_\mathrm{f})t_2+x_{t_2}-x_0), \tag{16}$$

and obtain the bivariate characteristic function φ_X^j, $j=N$, S, for $X=(x_{t_1},x_{t_2})$ under the measures $\mathbb{Q}_N$ and $\mathbb{Q}_S$ by

$$\varphi_X^j(u_1,u_2)=\mathbb{E}^{\mathbb{Q}_j}[\exp(iu_1x_{t_1}+iu_2x_{t_2})]. \tag{17}$$

The derivation of φ^N and φ^S is similar, since

$$\varphi_X^S(u_1,u_2)=\exp(-(r_\mathrm{d}-r_\mathrm{f})t_2-x_0)\mathbb{E}^{\mathbb{Q}_N}[\exp(iu_1x_{t_1} + i(u_2-i)x_{t_2})]. \tag{18}$$

We proceed with the derivation of φ^N.

The logarithmic spot price at time t_1, given the values x_0 and v_0, can be written as

$$\begin{aligned} x_{t_1} &= x_0+(r_\mathrm{d}-r_\mathrm{f})t_1-\frac{1}{2}\int_0^{t_1} v_t\,\mathrm{d}t+\int_0^{t_1}\sqrt{v_t}\,\mathrm{d}W_t^S \\ &= x_0+(r_\mathrm{d}-r_\mathrm{f})t_1-\frac{1}{2}\int_0^{t_1} v_t\,\mathrm{d}t \\ &\quad +\rho\int_0^{t_1}\sqrt{v_t}\,\mathrm{d}W_t^v+\rho_2\int_0^{t_1}\sqrt{v_t}\,\mathrm{d}W_t, \end{aligned} \tag{19}$$

where $\rho_2=\sqrt{1-\rho^2}$ and $\mathrm{d}W_t^S=\rho\mathrm{d}W_t^v+\rho_2\mathrm{d}W_t$ is the Cholesky decomposition of the Brownian motion W^S into the sum of W^v and another independent Brownian motion W.

The variance at time t_1 is given by the integral equation

$$v_{t_1}-v_0=\kappa\theta t_1-\kappa\int_0^{t_1} v_t\,\mathrm{d}t+\sigma\int_0^{t_1}\sqrt{v_t}\,\mathrm{d}W_t^v. \tag{20}$$

Invoking equation (20), we can replace the term $\int_0^{t_1}\sqrt{v_t}\,\mathrm{d}W_t^v$ in equation (19) by

$$\frac{1}{\sigma}\left[v_{t_1}-v_0-\kappa\theta t_1+\kappa\int_0^{t_1} v_t\,\mathrm{d}t\right].$$

Inserting the model definitions for x_{t_1} and x_{t_2} into (17), we derive

$$\begin{aligned} \varphi_X^N(u_1,u_2) &= \exp(iu_1h(t_1)+iu_2h(t_2)) \\ &\quad\times\mathbb{E}^{\mathbb{Q}_N}\Bigg[\exp\Bigg\{i(u_1+u_2)\Bigg(-\frac{1}{2}\int_0^{t_1} v_t\,\mathrm{d}t \\ &\quad+\frac{\rho}{\sigma}\left[v_{t_1}-j(t_1)+\kappa\int_0^{t_1} v_t\,\mathrm{d}t\right]+\rho_2\int_0^{t_1}\sqrt{v_t}\,\mathrm{d}W_t\Bigg) \\ &\quad+iu_2\Bigg(-\frac{1}{2}\int_{t_1}^{t_2} v_t\,\mathrm{d}t+\frac{\rho}{\sigma}\Bigg[v_{t_2}-v_{t_1}-\kappa\theta(t_2-t_1) \\ &\quad+\kappa\int_{t_1}^{t_2} v_t\,\mathrm{d}t]+\rho_2\int_{t_1}^{t_2}\sqrt{v_t}\,\mathrm{d}W_t\Bigg)\Bigg\}\Bigg], \end{aligned}$$

with h and j defined as in (9) and (10), respectively. Let $\sigma(W_s^v: 0\le s\le t_2)$ represent the filtration generated by $\{W_s^v\}_{t\le s\le t_2}$. In the following step, we take the conditional expectation value with respect to $\sigma(W_s^v: 0\le s\le t_2)$. Since all terms in the expectations are W^v-measurable except for those containing $iu_2\rho_2\int_{t_1}^{t_2}\sqrt{v_t}\,\mathrm{d}W_t$ and $i(u_1+u_2)\rho_2\int_0^{t_1}\sqrt{v_t}\,\mathrm{d}W_t$, we obtain

$$\begin{aligned} \varphi_X^N(u_1,u_2) &= \exp(iu_1h(t_1)+iu_2h(t_2)) \\ &\quad\times\mathbb{E}^{\mathbb{Q}_N}\Bigg[\exp\Bigg\{i(u_1+u_2)\Bigg(-\frac{1}{2}\int_0^{t_1} v_t\,\mathrm{d}t \\ &\quad+\frac{\rho}{\sigma}\left[v_{t_1}-j(t_1)+\kappa\int_0^{t_1} v_t\,\mathrm{d}t\right]\Bigg) \\ &\quad+iu_2\Bigg(-\frac{1}{2}\int_{t_1}^{t_2} v_t\,\mathrm{d}t+\frac{\rho}{\sigma}\Bigg[v_{t_2}-v_{t_1}-\kappa\theta(t_2-t_1) \\ &\quad+\kappa\int_{t_1}^{t_2} v_t\,\mathrm{d}t\Bigg]\Bigg)\Bigg\} \\ &\quad\times\mathbb{E}^{\mathbb{Q}_N}\Bigg[\exp\Bigg\{i\rho_2(u_1+u_2)\int_0^{t_1}\sqrt{v_t}\,\mathrm{d}W_t \\ &\quad+iu_2\rho_2\int_{t_1}^{t_2}\sqrt{v_t}\,\mathrm{d}W_t\Bigg\}\,\Bigg|\,\sigma(W_s^v: 0\le s\le t_2)\Bigg]\Bigg]. \end{aligned}$$

Given $\{W^v\}$, the path of v is known from time $t=0$ until t_2, and is therefore deterministic. It follows that the integrals $\int_0^{t_1}\sqrt{v_t}\,\mathrm{d}W_t$ and $\int_{t_1}^{t_2}\sqrt{v_t}\,\mathrm{d}W_t$ are normally distributed with zero mean. Since W^v and W are independent, the two integrals are also uncorrelated and therefore the random variables

$$\exp\left(i(u_1+u_2)\rho_2\int_0^{t_1}\sqrt{v_t}\mathrm{d}W_t\right) \quad\text{and}\quad \exp\left(iu_2\rho_2\int_{t_1}^{t_2}\sqrt{v_t}\mathrm{d}W_t\right)$$

are independent. Hence, the above expectation is equal to the product of the two single expectations of the two terms. The variances are calculated via the Itô isometry, and are equal to $\int_0^{t_1} v_t\,\mathrm{d}t$ and $\int_{t_1}^{t_2} v_t\,\mathrm{d}t$, respectively. Using the characteristic function for a normally distributed variable X, $\mathbb{E}[\mathrm{e}^{iaX}]=\mathrm{e}^{ia\mathbb{E}X-(1/2)a^2\mathrm{Var}X}$, the above yields

$$\begin{aligned} \varphi_X^N(u_1,u_2) &= \exp\Bigg(iu_1h(t_1)+iu_2h(t_2)-i(u_1+u_2)\frac{\rho}{\sigma}j(t_1) \\ &\quad-iu_2\frac{\rho}{\sigma}\kappa\theta(t_2-t_1)\Bigg) \\ &\quad\times\mathbb{E}^{\mathbb{Q}_N}\Bigg[\exp\Bigg\{iu_1\frac{\rho}{\sigma}v_{t_1}+iu_2\frac{\rho}{\sigma}v_{t_2} \\ &\quad+\left(-\frac{1}{2}+\kappa\frac{\rho}{\sigma}+\frac{1}{2}i(u_1+u_2)\rho_2^2\right) \\ &\quad\times i(u_1+u_2)\int_0^{t_1} v_t\,\mathrm{d}t+\left(-\frac{1}{2}+\kappa\frac{\rho}{\sigma}+\frac{1}{2}iu_2\rho_2^2\right)iu_2 \\ &\quad\times\int_{t_1}^{t_2} v_t\,\mathrm{d}t\Bigg\}\Bigg]. \end{aligned}$$

Using the functions p and q defined in (13) and (14), the characteristic function takes the form

$$\begin{aligned} \varphi_X^N(u_1,u_2) &= \exp(iu_1h(t_1)+iu_2h(t_2)-q(u_1)j(t_1)-q(u_2)j(t_2)) \\ &\quad\times\mathbb{E}^{\mathbb{Q}_N}\Bigg[\exp\Bigg\{q(u_1)v_{t_1}+q(u_2)v_{t_2} \\ &\quad+p(u_2)\int_{t_1}^{t_2} v_t\,\mathrm{d}t+p(u_1+u_2)\int_0^{t_1} v_t\,\mathrm{d}t\Bigg\}\Bigg]. \end{aligned}$$

Now we see that the characteristic function consists only of two types of random variables: the values of the variance at both times t_1 and t_2, and the time-integrals with respect to the paths of the variance process between 0 and t_1 and between t_1 and t_2. Therefore, using the tower property and taking out the terms that are known with respect to the information up to time t_1 results in

$$\varphi_X^N(u_1,u_2) = \exp(iu_1h(t_1) + iu_2h(t_2) - q(u_1)j(t_1) - q(u_2)j(t_2)) \times \mathbb{E}^{\mathbb{Q}_N}\left[\exp\left\{q(u_1)v_{t_1} + p(u_1+u_2)\int_0^{t_1} v_t\,\mathrm{d}t\right\} \times \mathbb{E}^{\mathbb{Q}_N}\left[\exp\left\{q(u_2)v_{t_2} + p(u_2)\int_{t_1}^{t_2} v_t\,\mathrm{d}t\right\}\middle|\mathcal{F}_{t_1}\right]\right].$$

We note that the calculation of $\varphi_X^N(u_1,u_2)$ is now reduced to that of the above nested expectations. The inner expectation

$$\mathbb{E}^{\mathbb{Q}_N}\left[\exp\left\{q(u_2)v_{t_2} + p(u_2)\int_{t_1}^{t_2} v_t\,\mathrm{d}t\right\}\middle|\mathcal{F}_{t_1}\right]$$

is solvable by application of the Feynman–Kac formula.

If we define the function $y(t,v_t)$ for a fixed time $0<t<t_2$ by

$$y(t,v_t) = \mathbb{E}^{\mathbb{Q}_N}\left[\exp\left\{q(u_2)v_{t_2} + p(u_2)\int_t^{t_2} v_s\mathrm{d}s\right\}\middle|\mathcal{F}_t\right],$$

the Feynman–Kac formula tells us that y must satisfy the partial differential equation

$$-\frac{\partial y}{\partial t} = p(u_2)vy + \kappa(\theta - v)\frac{\partial y}{\partial v} + \frac{1}{2}\sigma^2 v\frac{\partial^2 y}{\partial v^2},$$

with boundary condition

$$y(t_1, v_{t_1}) = \exp(q(u_2)v_{t_1}).$$

This partial differential equation is solvable if we assume that y is log-linear† and given by $y(t,v_t) = \exp[A(t_2-t)v_t + B(t_2-t)]$. Then the functions A and B must be of the form (11) and (12), respectively.

Inserting this solution into the outer expectation above, the characteristic function has the following structure:

$$\varphi_X^N(u_1,u_2) = \exp(iu_1h(t_1) + iu_2h(t_2) - q(u_1)j(t_1) - q(u_2)j(t_2))\exp(B(t_2-t_1,q(u_2),p(u_2))) \times \mathbb{E}^{\mathbb{Q}_N}\left[\exp\left\{\Big(q(u_1) + A(t_2-t_1,q(u_2),p(u_2))\Big)v_{t_1} + p(u_1+u_2)\int_0^{t_1} v_t\,\mathrm{d}t\right\}\right].$$

It remains to solve the outer expectation in $\varphi_X^N(u_1,u_2)$,

$$\begin{aligned}&\mathbb{E}^{\mathbb{Q}_N}\left[\exp\left\{(q(u_1) + A(t_2-t_1,q(u_2),p(u_2)))v_{t_1} + p(u_1+u_2)\int_0^{t_1} v_t\,\mathrm{d}t\right\}\right]\\ &= \exp[A(t_1,A_1,p(u_1+u_2))v_0 + B(t_1,A_1,p(u_1+u_2))]\\ &= \exp[A_2v_0 + B_2],\end{aligned}$$

where A_1, A_2 and B_2 are defined in equations (8) and (7).

Therefore, the joint characteristic function of $\ln S_{t_1}$ and $\ln S_{t_2}$ with respect to the probability measure $\mathbb{Q}_N$ is given by

$$\varphi_X^N(u_1,u_2) = \exp(i(u_1h(t_1) + u_2h(t_2)) - q(u_1)j(t_1) - q(u_2)j(t_2) + B_1 + B_2 + A_2v_0),$$

with the functions A_2, B_1 and B_2 defined as in (8) and (7).

By repeated application of the same principles as in the derivation above we can show by induction that the n-variate characteristic functions under the measures $\mathbb{Q}_N$ and $\mathbb{Q}_S$ of the log-spot vector $X=(x_{t_1},\ldots,x_{t_n})$ at times $0<t_1<\cdots<t_n=T$ for an arbitrary n are given by (6) and (15). □

Remark 2: The same idea can be used to derive multivariate characteristic functions dependent on n log-spot values and m volatility values.

Remark 3: The derivation of the n-variate characteristic functions can be adapted and transferred to a more general class of stochastic volatility models. Further examples of these kinds of models are the model of Zhu (2000), the Bates (SVJ) and SVCJ models of Duffie *et al.* (2000) and multidimensional Heston models such as the three-factor model of Dempster and Hong (2000) or the model developed by da Fonseca *et al.* (2005).

2.2. Applications of characteristic functions in option pricing

The result reported below in this section makes the important theoretical connection between characteristic functions and distribution functions in analytical form. This enables us to derive closed-form formulas in (in)complete models. We assume that the characteristic function φ is known, as in (6) and (15), and we wish to compute the distribution function F directly from it.

Theorem 2.2: (*Shephard*) *Let F denote the distribution function of interest. Suppose its corresponding density, f, is Lebesgue-integrable, $f\in L^n$, and its characteristic function $\varphi(u)\in L^n$. Then under the assumption of the existence of a mean for the random variable of interest, the following equality holds for $x=(x_1,\ldots,x_n)\in\mathbb{R}^n$:*

$$\begin{aligned}t(x) = {}&2^nF_{X_1,\ldots,X_n}(x_1,\ldots,x_n) - 2^{n-1}[F_{X_2,\ldots,X_n}(x_2,\ldots,x_n) + \cdots + F_{X_1,\ldots,X_{n-1}}(x_1,\ldots,x_{n-1})]\\ &+ 2^{n-2}[F_{X_3,\ldots,X_n}(x_3,\ldots,x_n) + \cdots + F_{X_1,\ldots,X_{n-2}} \times (x_1,\ldots,x_{n-2})] + \cdots + (-1)^n,\end{aligned}$$

where we define

$$t(x) = \frac{(-2)^n}{(2\pi)^n}\int_0^\infty\cdots\int_0^\infty \Delta_{u_1}\left[\cdots\Delta_{u_n}\left[\frac{\varphi(u)\mathrm{e}^{-ix^\perp u}}{iu_1\cdots iu_n}\right]\right]\mathrm{d}u, \tag{21}$$

with $u=(u_1,\ldots,u_n)^\perp$ and $\Delta_a\,[\eta(a)] = \eta(a)+\eta(-a)$.

†We set up the derivatives of y w.r.t. τ, v and v^2 and then solve the resulting Riccatti-type ordinary differential equations.

Proof: The proof is given by Shephard (1991). □

Remark 4: The result of theorem 2.2 can be specified for the cases of n being odd or even,

$$\Delta_{u_1}\left[\cdots\Delta_{u_n}\left[\frac{\varphi(u)\mathrm{e}^{-ix^{\perp}u}}{iu_1\cdots iu_n}\right]\right] = \begin{cases} 2i^{n-1}\Delta_{u_2}\left[\cdots\Delta_{u_n}\Im\left[\frac{\varphi(u)\mathrm{e}^{-ix^{\perp}u}}{u_1\cdots u_n}\right]\right], & \text{if } n \text{ is odd,}\\ 2i^{n}\Delta_{u_2}\left[\cdots\Delta_{u_n}\Re\left[\frac{\varphi(u)\mathrm{e}^{-ix^{\perp}u}}{u_1\cdots u_n}\right]\right], & \text{if } n \text{ is even.}\end{cases}$$

For an implementation it might be better to express it with respect to the real part

$$\Delta_{u_1}\left[\cdots\Delta_{u_n}\left[\frac{\varphi(u)\mathrm{e}^{-ix^{\perp}u}}{iu_1\cdots iu_n}\right]\right] = 2\Delta_{u_2}\cdots\Delta_{u_n}\Re\left[\frac{\varphi(u)\mathrm{e}^{-ix^{\perp}u}}{iu_1\cdots iu_n}\right].$$

These results indicate how to calculate an n-dimensional distribution function if the n-variate characteristic function is given: compute recursively all values for the marginal distribution functions and then the integral term in (21). In particular, by definition of the distribution function we are able to compute values for probabilities $\mathbb{P}(S_{t_1}\le c_1,\ldots,S_{t_n}\le c_n)$ with constant boundaries c_i, $i=1,\ldots,n$. All other probabilities such as $\mathbb{P}(S_{t_1}\ge c_1,\ldots,S_{t_n}\ge c_n)$ can also be calculated if we express the probability in terms of distribution functions F, for example

$$\begin{aligned}\mathbb{P}(S_{t_1}\ge c_1,\ldots,S_{t_n}\ge c_n) &= 1-\sum_{i=1}^{n}F_{S_{t_i}}(c_i)+\sum_{i,j}F_{S_{t_i},S_{t_j}}(c_i,c_j)\\ &\quad\pm\cdots\pm F_{S_{t_1},\ldots,S_{t_n}}(c_1,\ldots,c_n).\end{aligned}$$

Determining the probabilities of such events establishes the core problem for the valuation of weakly path-dependent options. For instance, the computation of probabilities $\mathbb{P}(S_{t_1}\le c_1,\ldots,S_{t_n}\le c_n)$ is part of the computation of the values of discretely monitored up-and-out options, where the distribution of the random variables $S_{t_1},\ldots,S_{t_n}$ is defined by the model at hand and determined by their joint characteristic function. Similarly, probabilities of the form $\mathbb{P}(S_{t_1}\ge c_1,\ldots,S_{t_n}\ge c_n)$ need to be calculated for the valuation of other options, such as discrete down-and-out options.

The above remarks show that the application of Shephard's theorem might be useful only for lower-dimensional problems. As the formula for an n-dimensional distribution function F contains all marginal distribution functions, it can be computationally time consuming to evaluate them with multidimensional numerical integration methods. Therefore, this method might only be suitable for the valuation of options that are dependent on a small number of random spot values. In the next section we will apply it for the case of fader options, a case where the payoff of the option depends on two random variables, $X_1=\ln S_t$ and $X_2=\ln S_T$ ($n=2$). Then the above statement yields the relationship

$$\begin{aligned}&\frac{2^2}{(2\pi)^2}\iint_0^{\infty}\Delta_{u_1}\left[\Delta_{u_2}\left[\frac{\varphi(u)\mathrm{e}^{-ix^{\perp}u}}{iu_1 iu_2}\right]\right]\mathrm{d}t_1\mathrm{d}t_2\\ &=\frac{-2^3}{(2\pi)^2}\iint_0^{\infty}\Delta_{u_2}\Re\left[\frac{\varphi(u)\mathrm{e}^{-ix^{\perp}u}}{u_1u_2}\right]\mathrm{d}u_1\mathrm{d}u_2\\ &=4F_{X_1,X_2}(x_1,x_2)-2[F_{X_1}(x_1)+F_{X_2}(x_2)]+1.\end{aligned}$$

Therefore, the distribution function F of X_1 and X_2 at (x_1,x_2) is given by

$$\begin{aligned}&F_{X_1,X_2}(x_1,x_2)\\ &=\frac{1}{4}-\frac{1}{2\pi}\int_0^{\infty}\Re\left[\frac{\varphi(u_1,0)\mathrm{e}^{-iu_1x_1}+\varphi(0,u_2)\mathrm{e}^{-iu_1x_2}}{iu_1}\right]\mathrm{d}u_1\\ &\quad-\frac{1}{2\pi^2}\iint_{\mathbb{R}_+^2}\Re\left[\frac{\left\{\begin{array}{l}\varphi(u_1,u_2)\mathrm{e}^{-iu_1x_1-iu_2x_2}\\ \quad-\varphi(u_1,-u_2)\mathrm{e}^{-iu_1x_1+iu_2x_2}\end{array}\right\}}{u_1u_2}\right]\mathrm{d}u_1\mathrm{d}u_2.\end{aligned}\tag{22}$$

The closed-form pricing formula for fader options is composed of these and similar probabilities.

Another possible application of the results of theorem 2.1 is using (fractional) fast Fourier transforms, as we will discuss in section 5.

3. Fader options

3.1. Introduction to fader options

A fader option is a plain vanilla option whose notional is determined by a fade-in (or fade-out) factor λ. This factor λ increases (decreases) for every time t_i where the spot fixing stays inside a given range $[L,H]$. If the spot never leaves the range, in the case of a fade-in option the payoff is a plain vanilla payoff with 100% of the notional accumulated. More formally, the payoff of a fade-in call at maturity T is given by

$$\lambda(S_T-K)^+,\quad\text{with }\lambda=\frac{1}{N}\sum_{i=1}^{N}\mathbb{1}_{\{S_{t_i}\in[L,H]\}},$$

where $0<t_1<\cdots<t_N=T$ is a set of fade-in dates within $[0,T]$. We take spot values at time t as the usual approximation of the fixing or closing price. The impact of this approximation is illustrated by Becker and Wystup (2009). For fade-out options, λ is replaced by $1-\lambda$.

The advantage of a fade-in option is that it is cheaper than the corresponding plain vanilla product. However, this kind of product needs the incorporation of a market view on the whole spot price path at times t_i. This market view may either be that λ is expected to be close to or smaller than 1. In the first case, the factor will not affect the payoff, but will affect the price of the product.

The valuation of fader options in the Black–Scholes model is explained by Overhaus *et al.* (1999) and Hakala and Wystup (2002). Various applications in structuring and variations and a trader's approach of how to price and hedge a fader option is covered by Wystup (2006).

Under the risk-neutral measure $\mathbb{Q}_N$, a fader option with strike price K and fixing times $t_1, \dots, t_n = T$ can be valued at time 0 in the context of equivalent martingale measures:

$$\begin{aligned} V_{\text{fader}}(K, L, H) &= \mathrm{e}^{-r_{\mathrm{d}}T}\mathbb{E}^{\mathbb{Q}_N}\left[(S_T - K)^+ \frac{1}{N}\sum_{i=1}^{N} \mathbb{1}_{\{S_{t_i}\in[L,H]\}}\right] \\ &= \frac{1}{N}\sum_{i=1}^{N} \underbrace{\mathrm{e}^{-r_{\mathrm{d}}T}\mathbb{E}^{\mathbb{Q}_N}[(S_T - K)^+ \mathbb{1}_{\{S_{t_i}\in[L,H]\}}]}_{=V_F(t_i)} \\ &= \frac{1}{N}\sum_{i=1}^{N} V_F(t_i). \end{aligned} \tag{23}$$

Therefore, the valuation of a fader option reduces to the determination of the discounted expectations in equation (23), denoted by $V_F(t)$, for $t \in \{t_1, \dots, t_N\}$. In the following section we first set up a pricing formula and then derive a closed-form solution for V_F in the Heston model for an arbitrary fixing time $t \le T$.

3.2. *Valuation of fader options in the Heston model*

With a change of notation to log-spot values $x_t = \ln S_t$, the value $V_F(t)$ at time 0, defined in equation (23), is given by

$$\begin{aligned} V_F(t) &= \mathrm{e}^{-r_{\mathrm{d}}T}\mathbb{E}^{\mathbb{Q}_N}[(S_T - K)^+ \mathbb{1}_{\{S_t\in[L,H]\}}] \\ &= \mathrm{e}^{-r_{\mathrm{d}}T}\mathbb{E}^{\mathbb{Q}_N}[(\mathrm{e}^{x_T} - K)\mathbb{1}_{\{l\le x_t\le h, k\le x_T\}}], \end{aligned}$$

and can be extended to the four expectations of indicator functions, so that

$$\begin{aligned} V_F(t) &= \mathrm{e}^{-r_{\mathrm{d}}T}[\mathbb{E}^{\mathbb{Q}_N}[\mathrm{e}^{x_T}\mathbb{1}_{\{x_t\le h, x_T\ge k\}}] - \mathbb{E}^{\mathbb{Q}_N}[\mathrm{e}^{x_T}\mathbb{1}_{\{x_t\le l, x_T\ge k\}}]] \\ &\quad - \mathrm{e}^{-r_{\mathrm{d}}T}K[\mathbb{E}^{\mathbb{Q}_N}[\mathbb{1}_{\{x_t\le h, x_T\ge k\}}] - \mathbb{E}^{\mathbb{Q}_N}[\mathbb{1}_{\{x_t\le l, x_T\ge k\}}]], \end{aligned} \tag{24}$$

where $k = \ln K$, $l = \ln L$ and $h = \ln H$. For the first two terms in (24), choose the spot price as numeraire and switch from probability measure $\mathbb{Q}_N$ to $\mathbb{Q}_S$. According to Girsanov's theorem, the relationship between the two measures $\mathbb{Q}_N$ and $\mathbb{Q}_S$ is given by the Radon–Nikodym derivative g_S as defined in equation (16).

Under this new measure, the option value representation can be restated as

$$V_F(t) = S_0\mathbb{E}^{\mathbb{Q}_S}[\mathbb{1}_{\{x_T\ge k, x_t\in[l,h]\}}] - \mathrm{e}^{-r_{\mathrm{d}}T}K\mathbb{E}^{\mathbb{Q}_N}[\mathbb{1}_{\{x_T\ge k, x_t\in[l,h]\}}].$$

The value of a fadlet $V_F(t)$ in (23), for some $t \in \{t_1, \dots, t_n\}$, can also be expressed in terms of four probabilities, so that

$$\begin{aligned} V_F(t) &= \mathrm{e}^{-r_{\mathrm{f}}T}S_0[\mathbb{Q}_S(x_T \ge k, x_t \le h) - \mathbb{Q}_S(x_T \ge k, x_t \le l)] \\ &\quad - \mathrm{e}^{-r_{\mathrm{d}}T}K[\mathbb{Q}_N(x_T \ge k, x_t \le h) - \mathbb{Q}_N(x_T \ge k, x_t \le l)]. \end{aligned} \tag{25}$$

In section 2, theorem 2.2 gives the representation of an n-distribution function F in terms of its marginal distribution functions. In the case of the fader option we see from equation (25) that we need to be able to compute probabilities of the form $\mathbb{P}(x_t \le c_1,\ x_T \ge c_2)$, for some constants c_1 and c_2, with respect to the measures $\mathbb{Q}_N$ and $\mathbb{Q}_S$ in order to price fader options in the Heston model. We apply Shephard's theorem 2.2 for $n = 2$ (see also equation (22)) to obtain an expression for the two-dimensional distribution function $F(c_1, c_2)$ with respect to $\mathbb{Q}_j$, $j = N, S$, which is equal to

$$\begin{aligned} &F_j(h,k) \\ &= \frac{1}{4} - \frac{1}{2\pi}\int_0^\infty \Re\left[\frac{\varphi_j(0,u_2)\mathrm{e}^{-iu_2k}}{iu_2}\right]\mathrm{d}u_2 \\ &\quad - \frac{1}{2\pi}\int_0^\infty \Re\left[\frac{\varphi_j(u_1,0)\mathrm{e}^{-iu_1h}}{iu_1}\right]\mathrm{d}u_1 \\ &\quad - \frac{1}{2\pi^2}\iint_{\mathbb{R}_+^2} \Re\left[\frac{\left\{\begin{array}{l}\varphi_j(u_1,u_2)\mathrm{e}^{-iu_1h-iu_2k} \\ -\varphi_j(u_1,-u_2)\mathrm{e}^{-iu_1h+iu_2k}\end{array}\right\}}{u_1u_2}\right]\mathrm{d}u_1\mathrm{d}u_2. \end{aligned}$$

Since the joint distribution function $F(c_1, c_2)$ of a random vector $X = (X_1, X_2)$ is defined by the probability $\mathbb{P}(X_1 \le c_1, X_2 \le c_2)$, we can express the probability $\mathbb{P}(X_1 \le c_1, X_2 \ge c_2)$ in terms of distribution functions:

$$\begin{aligned} F^*(c_1,c_2) &= \mathbb{P}(X_1 \le c_1, X_2 \ge c_2) \\ &= \mathbb{P}(X_1 \le c_1) - \mathbb{P}(X_1 \le c_1, X_2 \le c_2) \\ &= F(c_1) - F(c_1,c_2). \end{aligned} \tag{26}$$

From (26), we obtain the desired probabilities using

$$\begin{aligned} &F_j^*(h,k) \\ &= \frac{1}{4} + \frac{1}{2\pi}\int_0^\infty \Re\left[\frac{\varphi_j(0,u_2)\mathrm{e}^{-iu_2k}}{iu_2}\right]\mathrm{d}u_2 \\ &\quad - \frac{1}{2\pi}\int_0^\infty \Re\left[\frac{\varphi_j(u_1,0)\mathrm{e}^{-iu_1h}}{iu_1}\right]\mathrm{d}u_1 \\ &\quad + \frac{1}{2\pi^2}\iint_{\mathbb{R}_+^2} \Re\left[\frac{\left\{\begin{array}{l}\varphi_j(u_1,u_2)\mathrm{e}^{-iu_1h-iu_2k} \\ -\varphi_j(u_1,-u_2)\mathrm{e}^{-iu_1h+iu_2k}\end{array}\right\}}{u_1u_2}\right]\mathrm{d}u_1\mathrm{d}u_2, \end{aligned}$$

which is obtained by an application of Shephard's theorem. Finally, the value of a fader call option at time $t = 0$ in the Heston model is given by

$$\begin{aligned} V_{\text{fader}}(K,L,H) &= \frac{1}{N}\sum_{i=1}^{N} V_F(t_i), \quad \text{with} \\ V_F(t_i) &= S_0\mathrm{e}^{-r_{\mathrm{f}}T}[F_2^*(h,k) - F_2^*(l,k)] \\ &\quad - K\mathrm{e}^{-r_{\mathrm{d}}T}[F_1^*(h,k) - F_1^*(l,k)]. \end{aligned} \tag{27}$$

The corresponding characteristic functions are defined in (6) and (15) by setting n equal to 2. The value of a fader put option can be derived in an equivalent manner.

Note that equation (27) is model independent (within the context of complete models). The calculation of a fader option value within a specific model can be accomplished by calculating the appropriate characteristic functions for $\ln S_t$. For example, to price a fader option in the Black–Scholes model, choose the bivariate characteristic function for normally distributed random variables. To price it in the Heston model, express F_1^* and F_2^* with respect to the characteristic functions (6) and (15).

Remark 5: Equation (27) specifies the value of a fader call at time 0 with respect to some underlying distribution of log-spot values and constant market data r_d, r_f, constant contract data K, L, H and constant model parameters. This formula can be extended to a valuation formula for fader options where these data are time-dependent, for example as step functions taking constant values between fixing times.

4. Discretely monitored barrier options

4.1. *Introduction to discretely monitored barrier options*

One further application of the n-variate characteristic functions is the valuation of discretely monitored barrier options in the Heston model. Barrier options where the barriers are monitored only at finitely many fixed time points are called discretely monitored barrier options in contrast to continuously monitored barrier options, where the barrier is valid at all times between trade time and maturity. In the case of a discretely monitored barrier option with strike K, constant barrier H and maturity T, the payoffs are given by

$$(\phi(S_T-K))^+\mathbb{1}_{\{\max_{i\in\{1,..n\}}S_{t_i}<H\}},$$
$$(\phi(S_T-K))^+\mathbb{1}_{\{\max_{i\in\{1,..n\}}S_{t_i}>H\}},$$
$$(\phi(S_T-K))^+\mathbb{1}_{\{\min_{i\in\{1,..n\}}S_{t_i}<H\}},$$
$$(\phi(S_T-K))^+\mathbb{1}_{\{\min_{i\in\{1,..n\}}S_{t_i}>H\}},$$

where $\phi=\pm1$ is a put/call indicator taking the value $+1$ in the case of a call and -1 in the case of a put, $0<t_1<\cdots<t_n=T$ is a finite set of barrier monitoring times for the underlying in the time interval $[0, T]$ and T the maturity of the option. The four payoffs above define the payoffs for so-called up-and-out, up-and-in, down-and-in and down-and-out options. For calls we abbreviate these payoff functions by UOC, DOC, DIC and UIC, respectively. This notation will also be used to denote the value of the option.

Before going into detail, let us point out the following relations between the payoffs of barrier options and vanilla options. The in–out parity for barrier options, namely knock-in+knock-out = vanilla, allows us to consider only the family of knock-out options for the derivation of closed-form formulas, since a closed-form formula for vanilla options in the Heston model already exists. Additionally, since the well-known symmetry relation between call and put options in the Black–Scholes model can be derived in similar form in the Heston model for discrete barrier options in an FX context, it is sufficient to treat only calls. Hence, we give details only for knock-out call options. In order to be able to price all types of barrier options, i.e. knock-in calls and puts and knock-out calls and puts, altogether, we need to examine three types of payoff functions.

- Down-and-out: For $H<S_0$,

$$(S_T-K)\mathbb{1}_{\{H\le S_{t_1},\ldots,H\le S_{t_n}\}},\qquad \text{for } K<H,$$
$$(S_T-K)\mathbb{1}_{\{H\le S_{t_1},\ldots,H\le S_{t_{n-1}},K\le S_{t_n}\}},\qquad \text{for } H<K.$$

- Up-and-out: For $S_0<H$ and $K<H$,

$$(S_T-K)\mathbb{1}_{\{H\ge S_{t_1},\ldots,H\ge S_{t_{n-1}},K\le S_{t_n}\le H\}}.$$

Remark 6: More generally, for each fixed barrier monitoring time t_i there can be a different barrier level H_i. The payoff of an up-and-out call option, for example, then changes to

$$(S_T-K)^+\mathbb{1}_{\{S_{t_1}<H_1,S_{t_2}<H_2,\ldots,S_{t_n}<H_n\}}.$$

Here we choose all barriers to be equal for simplicity and easier implementation, but of course all the arguments hold also for varying barrier levels H_i.

4.2. *Valuation of discrete barrier options in the Heston model*

We can rewrite the value of an up-and-out barrier call option,

$$V_{\mathrm{UOC}}=\mathrm{e}^{-r_dT}\mathbb{E}^{\mathbb{Q}_N}[(\mathrm{e}^{x_T}-K)\mathbb{1}_{\{x_T>k\}}\mathbb{1}_{\{x_{t_1}<h,\ldots,x_{t_n}<h\}}],\tag{28}$$

as

$$\begin{aligned}V_{\mathrm{UOC}}&=\mathrm{e}^{-r_fT}S_0\mathbb{E}^{\mathbb{Q}_S}[\mathbb{1}_{\{x_T>k,x_{t_1}<h,\ldots,x_{t_n}<h\}}]\\&\quad-\mathrm{e}^{-r_dT}K\mathbb{E}^{\mathbb{Q}_N}[\mathbb{1}_{\{x_T>k,x_{t_1}<h,\ldots,x_{t_n}<h\}}]\\&=\mathrm{e}^{-r_fT}S_0[\mathbb{Q}_S(x_{t_1}<h,\ldots,x_{t_n}<h)\\&\quad-\mathbb{Q}_S(x_{t_1}<h,\ldots,x_{t_{n-1}}<h,x_{t_n}<k)]\\&\quad-\mathrm{e}^{-r_dT}K[\mathbb{Q}_N(x_{t_1}<h,\ldots,x_{t_n}<h)\\&\quad-\mathbb{Q}_N(x_{t_1}<h,\ldots,x_{t_{n-1}}<h,x_{t_n}<k)],\end{aligned}\tag{29}$$

using the measures $\mathbb{Q}_N$ and $\mathbb{Q}_S$ as defined in section 3 and the notation $h=\ln H$ and $k=\ln K$.

Again, this formula is independent of the model of the underlying dynamics of S (with respect to an equivalent martingale measure). By choosing a (in)complete model, one defines the distribution of S and therefore the values for the probabilities of the events in equation (29). In the Heston model the values for the probabilities in equation (29) can be calculated using the n-variate characteristic functions of section 2. As mentioned in section 2, the evaluation of these probabilities or, equivalently, these n-multiple integrals can be done by using the result of Shephard's theorem 2.2 and multidimensional numerical integration. For the calculation of discrete barrier option values, we reformulate theorem 2.2.

Corollary 4.1: *Let F denote the distribution function of interest and the integral term $t(\cdot)$ is defined as in equation* (21). *Assume the requirements of theorem* 2.2 *hold, then*

$$2F(x_1) = t(x_1) + 1, \quad \textit{for } n = 1,$$
$$4F(x_1, x_2) = t(x_1, x_2) + t(x_1, 0) + t(0, x_2) + 1, \quad \textit{for } n = 2,$$
$$2^n F(x_1, \ldots, x_n) = t(x_1, \ldots, x_n) + \sum_{j_1 < \cdots < j_{n-1}, 0 \le j_i \le n} t(x_{j_1}, \ldots, x_{j_{n-1}}, 0) + \cdots + \sum_j t(x_j) + 1, \quad \textit{for } n > 2.$$

Therefore, for the case of an up-and-out option we need to calculate probabilities of the form $\mathbb{P}(X_1 \le x_1, \ldots, X_n \le x_n) = F(x_1, \ldots, x_n)$ and can use corollary 4.1 directly.

For the case of a down-and-out option we need to calculate probabilities of the form $\mathbb{P}(X_1 \ge x_1, \ldots, X_n \ge x_n)$. In terms of distribution functions this means evaluating the terms

$$\mathbb{P}(X_1 \ge x_1, \ldots, X_n \ge x_n) = 1 - \sum_{j=1}^{n} F(x_j) + \sum_{i<j} F(x_i, x_j) \pm \cdots + (-1)^n F(x_1, \ldots, x_n). \tag{30}$$

With corollary 4.1 this yields

$$\begin{aligned}(30) &= 1 - \frac{1}{2}\sum_{j=1}^{n}(t(x_j) + 1) + \frac{1}{4}\sum_{i<j}(t(x_i, x_j) + t(x_i) \\ &\quad + t(x_j) + 1) \pm \cdots \pm (-1)^n \frac{1}{2^n}\Bigg(t(x_1, \ldots, x_n) \\ &\quad + \sum_{j_1 < \cdots < j_{n-1}, 0 \le j_i \le n} t(x_{j_1}, \ldots, x_{j_{n-1}}) + \cdots + \sum_{j=1}^{n} t(x_j) + 1\Bigg) \\ &= \frac{1}{2^n}\Bigg(1 - \sum_{j=1}^{n} t(x_j) + \sum_{i<j} t(x_i, x_j) \pm \cdots \\ &\quad + (-1)^n t(x_1, \ldots, x_n)\Bigg).\end{aligned}$$

Consequently, for the computation of discrete knock-out option values with n fixings, we need to be able to approximate $2^n - 1$ multi- or one-dimensional integrals numerically. We see that we must find a fast method to calculate n-dimensional distribution functions with respect to their characteristic functions.

In the following section we use and compare this technique with the fast Fourier transform approach, which gives us a general method to compute values of all types of discrete barrier options.

5. Computational issues

We begin with the implementational aspects for the computation of fader and discrete barrier option values using fast Fourier transform (FFT) methods. We follow the approach of Carr and Madan, established for European-style vanilla options in the one-dimensional case of Carr and Madan (1999) and the FFT algorithm of Dempster and Hong (2000) for the correlation option. We describe in detail how to apply the FFT method for vanilla option valuation to the case of multivariate characteristic functions and thereby the approximation of n-fold integrals. We then introduce the Monte Carlo sampling scheme as a comparison. We mainly compare the obtained results with respect to computational accuracy.

5.1. *Implementational aspects of the fast Fourier transform method*

In order to evaluate option pricing formulas, such as (23) and (28), we describe a general technique of fast Fourier transforms for options with payoff functions that are dependent on n different spot values in time. As a case study we treat a discrete down-and-out barrier call option with upper barrier level $K < H$,

$$V_{\mathrm{DOC}} = \mathbb{E}^{\mathbb{Q}_N}\left[\mathrm{e}^{-r_\mathrm{d} t_n}(S_{t_n} - K)^+ \prod_{i=1}^{n} \mathbb{1}_{\{H \le S_{t_i}\}}\right] \tag{31}$$

$$= \mathbb{E}^{\mathbb{Q}_N} t[\mathrm{e}^{-r_\mathrm{d} t_n}(S_{t_n} - K)\mathbb{1}_{\{H \le S_{t_1}, \ldots, H \le S_{t_n}\}}]. \tag{32}$$

The above expectation (31) can be calculated in integral form as

$$E(k, h) = \int_h^\infty \cdots \int_h^\infty \mathrm{e}^{-r_\mathrm{d} t_n}(\mathrm{e}^{x_{t_n}} - e^k) q(x_{t_1}, \ldots, x_{t_n}) \mathrm{d}x_{t_n} \ldots \mathrm{d}x_{t_1}, \tag{33}$$

where the logarithms of the strike, barriers and spots K, H and S_{t_i} are denoted by k, h and x_{t_i}. In the case of $H < K$, the lower integration bound of the inner-most integral in (31) would be k instead of h and similarly for UOC options the equivalent of (33) is

$$\int_{-\infty}^{h} \cdots \int_{-\infty}^{h} \mathrm{e}^{-r_\mathrm{d} t_n}(\mathrm{e}^{x_{t_n}} - e^k) q(x_{t_1}, \ldots, x_{t_n}) \mathrm{d}x_{t_n} \mathrm{d}x_{t_{n-1}} \ldots \mathrm{d}x_{t_1}, \tag{34}$$

$$- \int_{-\infty}^{h} \cdots \int_{-\infty}^{h} \int_{-\infty}^{k} \mathrm{e}^{-r_\mathrm{d} t_n}(\mathrm{e}^{x_{t_n}} - e^k) q(x_{t_1}, \ldots, x_{t_n}) \mathrm{d}x_{t_n} \times \mathrm{d}x_{t_{n-1}} \ldots \mathrm{d}x_{t_1}, \tag{35}$$

where $\mathbb{Q}_N$ denotes the risk-neutral measure and $q(\cdot)$ the corresponding joint density of the random values x_{t_i}'s for given values x_0 and v_0.

As in Carr and Madan (1999) and Dempster and Hong (2000), $E(k, h)$ is multiplied by an exponentially decaying term $\exp(\alpha_1 h + \cdots + \alpha_n h)$, for $\alpha_i > 0$, so that it is square-integrable in h over the negative axes. Again, note that, for the case of $H < K$, the decaying term of α_n is formed with k instead of h.

The Fourier transform

$$\psi(v_1, \ldots, v_n) = \int_{\mathbb{R}^n} \mathrm{e}^{i(v_1 h + \cdots + v_n h)} \mathrm{e}^{\alpha_1 h + \cdots + \alpha_n h} E(k, h) \mathrm{d}h$$

of this modified integral can be expressed in terms of the characteristic function φ. The expression for $E(k, h)$ is inserted and the calculation proceeds similarly as in the one-dimensional case for vanilla options in Carr and Madan (1999). Because the characteristic function is known in closed form, the Fourier transform ψ will also be available analytically in terms of φ. Let $\tilde{v}_j$ denote $v_j - i\alpha_j$, then for $j = 1, \ldots, n$ we obtain the following.

- For the down-and-out call with $K < H$,

$$\psi(v_1, \ldots, v_n) = \mathrm{e}^{-r_{\mathrm{d}} t_n} \frac{\varphi(\tilde{v}_1, \ldots, \tilde{v}_{n-1}, \tilde{v}_n - i) - e^k \varphi(\tilde{v}_1, \ldots, \tilde{v}_n)}{i \prod_{j=1}^n \tilde{v}_j}. \tag{36}$$

- For the down-and-out call with $H < K$,

$$\psi(v_1, \ldots, v_n) = \mathrm{e}^{-r_{\mathrm{d}} t_n} \frac{\varphi(\tilde{v}_1, \ldots, \tilde{v}_{n-1}, \tilde{v}_n - i)}{(i\tilde{v}_n + 1) i \prod_{j=1}^n \tilde{v}_j}.$$

From the inverse Fourier transform, the integral $E(k, h)$ can be calculated using

$$E(k, h) = \frac{\mathrm{e}^{-\sum_{j=1}^n \alpha_j h}}{(2\pi)^n} \int_{\mathbb{R}^n} \mathrm{e}^{-i \sum_j v_j h} \psi(v_1, \ldots, v_n) \mathrm{d}v_n \cdots \mathrm{d}v_1. \tag{37}$$

For the fader option we can use (37) with $n = 2$. For the first integral term of the value of the up-and-out call in (34) we can use (36) and we can use (37) for the second integral term (35), both with negative arguments in the characteristic function. Furthermore, in this case, we choose the dampening parameter such that $\alpha > 1$, and set up the input array of the fast Fourier transform routine as a call of a Fourier transform (not the inverse Fourier transform) of the up-and-out call option, i.e.

$$(36) = \frac{\exp(\alpha_1 h + \cdots + \alpha_n h)}{(2\pi)^n} \int_{\mathbb{R}^n} \mathrm{e}^{i(v_1 + \cdots + v_n)h} \psi_1(v_1, \ldots, v_n) \mathrm{d}v$$

and

$$(37) = \frac{\exp(\alpha_1 h + \cdots + \alpha_n k)}{(2\pi)^n} \int_{\mathbb{R}^n} \mathrm{e}^{i(v_1 + \cdots + v_{n-1})h + i v_n k} \times \psi_2(v_1, \ldots, v_n) \mathrm{d}v,$$

with the corresponding Fourier transforms

$$\psi_1(v_1, \ldots, v_n) = \mathrm{e}^{-r_{\mathrm{d}} t_n} \frac{\varphi(-\tilde{v}_1, \ldots, -\tilde{v}_{n-1}, -\tilde{v}_n - i) - \mathrm{e}^k \varphi(-\tilde{v}_1, \ldots, -\tilde{v}_n)}{i \prod_{j=1}^n \tilde{v}_j},$$

$$\psi_2(v_1, \ldots, v_n) = -\mathrm{e}^{-r_{\mathrm{d}} t_n} \frac{\varphi(-\tilde{v}_1, \ldots, -\tilde{v}_{n-1}, -\tilde{v}_n - i)}{(i\tilde{v}_n - 1) i \prod_{j=1}^n \tilde{v}_j}.$$

Invoking the trapezoidal rule, the Fourier integral in (37) is approximated by the n-fold sum

$$E(k, h) \approx \frac{\mathrm{e}^{-\sum_{j=1}^n \alpha_j h}}{(2\pi)^n} \prod_j \Delta_j \underbrace{\sum_{m_1=0}^{N-1} \cdots \sum_{m_n=0}^{N-1} \mathrm{e}^{-i \sum_{j=1}^n v_{j,m_j} h} \psi(v_{1,m_1}, \ldots, v_{n,m_n})}_{=\Gamma(k)}, \tag{38}$$

where Δ_j denotes the integration step width and

$$v_{j,m_j} = \left(m_j - \frac{1}{2}N\right)\Delta_j, \quad \text{for } m_j = 0, \ldots, N-1.$$

Let the n-fold sums dependent on the n barrier levels h be denoted by $\Gamma\,(h, \ldots, h)$.

In order to apply the algorithm of fast Fourier transforms to evaluate the sums in equation (38), we define a grid of size N^n by $\Lambda = \{(h_{1,p_1}, \ldots, h_{n,p_n}) \mid 0 \le p_j \le N - 1\}$, where the coordinates are given by

$$h_{j,p_j} = p_j \lambda_j - \frac{1}{2} N \lambda_j + h, \quad \text{for } j = 1, \ldots, n.$$

In the case of a down-and-out discrete barrier call with $H < K$, the grid on the last random variable must be $h_{n,p_n} = p_n \lambda_n - \frac{1}{2} N \lambda_n + k$. Choosing $\lambda_1 \Delta_1 = \cdots = \lambda_n \Delta_n = 2\pi/N$ gives the following values of the n-fold sums $\Gamma(\cdot)$ on the grid Λ:

$$\Gamma(h_{1,p_1}, \ldots, h_{n,p_n}) = \sum_{m_1=0}^{N-1} \cdots \sum_{m_n=0}^{N-1} \mathrm{e}^{-i \sum_{j=1}^n v_{j,m_j} h_{j,p_j}} \times \psi(v_{1,m_1}, \ldots, v_{n,m_n}).$$

This can be computed with the fast Fourier transform by taking the input array as

$$X[m_1, \ldots, m_n] = (-1)^{\sum_{j=1}^n m_j} \mathrm{e}^{-i \sum_{j=1}^n h(m_j \Delta_j - (1/2) N \Delta_j)} \times \psi(v_{1,m_1}, \ldots, v_{n,m_n}),$$

such that

$$\Gamma(h_{1,p_1}, \ldots, h_{n,p_n}) = (-1)^{\sum_{j=1}^n p_j} \sum_{m_1=0}^{N-1} \cdots \sum_{m_n=0}^{N-1} \mathrm{e}^{-\sum_{j=1}^n (2\pi i/N) p_j m_j} X[m_1, \ldots, m_n]. \tag{39}$$

The result of the FFT algorithm is an output array Y that contains values for the n-fold sums in equation (39) at N^n different logarithmic barrier levels (or logarithmic strike values). The desired approximation of the price of the discrete barrier option is given by the real part of the complex number in Y, which is stored at $Y[\frac{1}{2}N, \ldots, \frac{1}{2}N]$. It follows that

$$V_{\mathrm{DOC}} \approx \frac{\mathrm{e}^{-\sum_{j=1}^n \alpha_j h}}{(2\pi)^n} (-1)^{(1/2)nN} \prod_j \Delta_j \times Y\left[\frac{1}{2}N, \ldots, \frac{1}{2}N\right].$$

Remark 7: Characteristic functions typically have an analytic extension $u \to z \in \mathbb{C}$, regular in some strip parallel to the real z axis. This aspect plays an import role in the application of fast Fourier transform methods to price options. Hence, to be able to apply the derived n-variate characteristic functions for a numerical analysis of option values within the above FFT methods, we need to make sure during the computations that the expected value $\mathbb{E}[\exp(iux)]$, for $u \in \mathbb{C}$, exists. Lee (2004) and Kahl and Lord (2010) analysed this issue of moment stability for the univariate characteristic function that is used in the closed-form formula for vanilla options in the Heston model.

5.2. *A sampling approach in the Heston model*

As mentioned in the introduction, there is recent literature dealing with the development of Monte Carlo schemes to sample from the asset price process following the Heston model dynamics. They all have the common goal of maintaining the speed of simulation with a Euler scheme, circumventing the problem of sampling negative variance values and still achieving the desired accuracy in option prices.

In this article, our focus is mainly on proposing a benchmark procedure for all these newly developed numerical methods with respect to accuracy in weakly path-dependent option prices and to a lesser extend with respect to computational time. Consider the pricing of exotic options in the Heston model using a numerical method of choice. In order to validate its correctness empirically, in the first instance one might certify that the prices for plain vanilla options obtained with this specific numerical method and the (semi-)analytical valuation formula coincide for a variety of representative model parameter sets. The closed-form formula in (3) might not be the fastest method to compute vanilla option prices, but it can be used to benchmark other pricing methods. In a step-by-step approach, the semi-analytical formulas derived in sections 3 and 4 can be used to benchmark a numerical method for weakly path-dependent financial products.

Hence, in order to choose Monte Carlo-type simulation scheme with which to compare our analytical approach, we decided to act on the following very simple suggestion. We discretize the time space with respect to an equidistant grid, $\{t_i\}_{i=1,\ldots,fn}$, where $t_i = i\Delta_t$ and $\Delta_t = T/(fn)$, including the corresponding fixing times of the product to be priced with a monitoring frequency of f. For instance, for a fader option with one year to maturity and a monthly fixing we use a grid with a multiple number n of 12 time points, $\{t_i\}_{i=1,\ldots,12n}$, where $t_i = i/(12n)$ and where $\{t_i\}_{i=1,n,2n,\ldots,12n}$ are the fade-in or fade-out times.

Now, for each time step t_i we sample the variance process v_{t_i} according to the non-central chi-squared distribution (let χ^2 be a non-central chi-squared r.v.) using

$$v_{t_i} = \frac{\sigma^2(1-\mathrm{e}^{-\kappa\Delta_t})}{4\kappa} \times \chi^2_R(\arg), \tag{40}$$

where $R = 4\kappa\theta/\sigma^2$ specifies the number of degrees of freedom and $\arg = 4\kappa\mathrm{e}^{-\kappa\Delta_t}/(\sigma^2(1-\mathrm{e}^{-\kappa\Delta_t})) \times v_{t_{i-1}}$ is the non-centrality parameter of the distribution.

On the other hand, discretization of the variance process in (1) with a Euler scheme leads to

$$v_{t_i} = v_{t_{i-1}} + \kappa(\theta - v_{t_{i-1}})\Delta_t + \sigma\sqrt{v_{t_{i-1}}}Z^v\sqrt{\Delta_t},$$

where the random variable Z^v is standard normally distributed. Hence, Z^v is given by

$$Z^v = \frac{v_{t_i} - v_{t_{i-1}} - \kappa(\theta - v_{t_{i-1}})\Delta_t}{\sigma\sqrt{v_{t_{i-1}}\Delta_t}}, \tag{41}$$

and if Δ_t is chosen too large, then the probability of sampling negative variance values increases.

In this approach we are not sampling Z^v itself, but v_{t_i}, as in (40). With a given v_{t_i} we calculate the right-hand side of equation (41). Let $\tilde{Z}^v$ denote the random variable generated in that way. Since all the quantities of the right-hand side of equation (41) are deterministic at that time t_{i-1}, except for v_{t_i}, the random variable $\tilde{Z}^v$ is non-central chi-squared distributed, but must be standard normally distributed in the limit.

To ensure that the random variable $\tilde{Z}_v$ is approximately normally distributed we compare its empirical distribution with the standard normal distribution after the first time step and adapt the grid width Δ_t accordingly. In that way, we circumvent the problem of sampling negative variances.

From here we proceed as usual, meaning we sample an independent normal random variable Z and sample for the logarithmic spot value at time t_i by

$$x_{t_i} = x_{t_{i-1}} + \left(r_\mathrm{d} - r_\mathrm{f} - \frac{1}{2}v_{t_{i-1}}\right)\Delta_t + \sqrt{v_{t_{i-1}}\Delta_t}(\rho\tilde{Z}^v + \sqrt{1-\rho^2}Z).$$

For each monitoring date the specific path-dependent condition of the option is checked and the discounted expected payoff at maturity is estimated by averaging over all simulated paths.

5.3. *Discussion of numerical results*

In this section we examine in detail the pricing of fader options and discretely monitored barrier options. We give some examples of sets of model parameters and compare the computation of the pricing values of the above financial products under different numerical methods. Therefore, numerical methods such as Monte Carlo simulation, fast Fourier transform and multidimensional numerical integration are implemented in C# and MatLab and applied to the described valuation problems.

The stability of the characteristic functions φ^N and φ^S is relevant for the application of the FFT method and also for the numerical integration. As discussed by Albecher *et al.* (2007) and Kahl and Lord (2010) there exist two representations of the univariate characteristic function $\ln S_T$ in the Heston model. Only one of them shows continuous behavior for all possible model parameters and makes it possible to use implementations of the multi-valued complex logarithm function which calculates only the principal value. Note that the marginal characteristic functions $\varphi_{x_{t_1},\ldots,x_{t_n}}(u_1,\ldots,u_n)$ are continuous as well and can be integrated without a rotation count algorithm due to the results concerning the univariate characteristic function of Albecher *et al.* (2007). For the multivariate case the problem of integrating a multi-valued complex logarithm in several dimensions still needs to be addressed.

In order to be able to use Monte Carlo simulation with a Euler discretization scheme and to compare the values obtained with the different numerical techniques, we decided to use the sampling technique described in section 5.2. Another possibility would be to especially

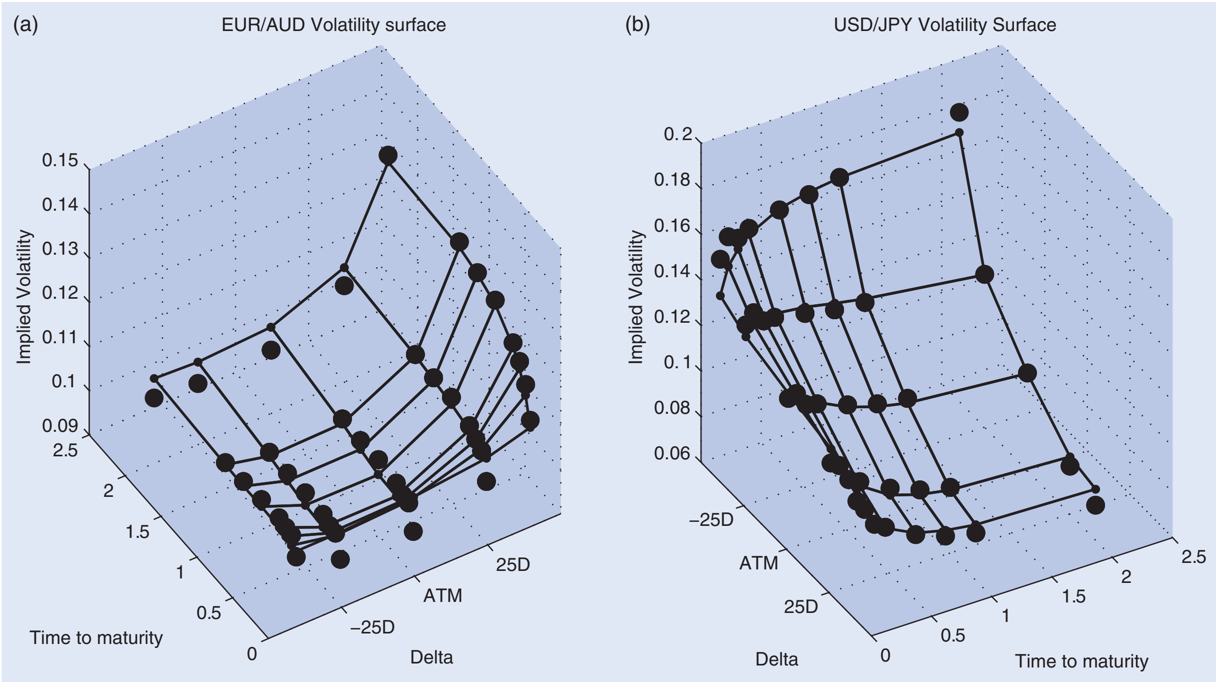

Figure 1. Implied volatilities of the Heston model fitted to market volatilities for an FX rate with maturities of 1, 2, 3, 6, 9, 12 and 24 months and strikes for 10%Δ and 25%Δ put, ATM, 25%Δ and 10%Δ call. (•) Market volatilities. The grid shows the calibrated volatilities. Left: EUR/AUD volatility surface. Right: USD/JPY volatility surface.

choose the sets of model parameters such that the probability of a negative variance on a discrete time grid is low.

Nevertheless, the methods using the multivariate characteristic functions are applicable for all combinations of model parameters, if multidimensional integration is applied.

Using numerical integration we have the choice of computing option values either with the formula given in equation (33), which is expressed with respect to the density function of n logarithmic spot values, or with the formulas for faders and discrete barriers derived in sections 3 and 4, which is defined with respect to the characteristic function of n logarithmic spot values. To determine the density function we need to compute the inverse Fourier transform of the characteristic function. A third option would be to use (37). The quality of the direct computation of (37) depends on the choice of the damping factors α_j, for $j = 1, \ldots, n$. Therefore, basically the core of all approaches can be found in the characteristic function. The only difference is the method for calculating the integrals defining the knock-out probabilities.

To use fast Fourier transform methods, we note that an extension of the multivariate characteristic functions for complex arguments might not be regular for all model parameters.

5.3.1. Two FX market data scenarios. For our subsequent computations we utilize two market data scenarios taken from FX market data, supplied by SuperDerivatives.† Therefore, we fitted implied volatilities of the Heston model to market volatilities of the EUR/AUD and USD/JPY exchange rates with maturities between 1 and 24months and strikes for 10%Δ and 25%Δ put, ATM, 25%Δ and 10%Δ call (figure 1). The calibration results for each scenario are given in tables 1 and 2.

Table 1. Parameter settings for the EUR/AUD market scenario.

Model parameters				
κ	θ	ρ	σ	v_0
2.6032	0.0138	0.1558	0.3802	0.0117
Market data				
S_0	r_d	r_f		
1.6411	0.0838	0.0503		

The EUR/AUD market scenario represents a market situation with a high speed of mean reversion as well as a high volatility of variance and a lower level of mean reversion and initial volatility. In particular, the EUR/AUD market scenario provides us with an example of a model parameter set that features a positive correlation parameter, whereas the USD/JPY market scenario describes a market where the correlation

†SuperDerivatives is an internet-based pricing tool for exotic options and a market data provider; see http://www.superderivatives.com

Table 2. Parameter settings for the USD/JPY market scenario.

Model parameters				
κ	θ	ρ	σ	v_0
0.7356	0.0164	−0.7309	0.3311	0.0165
Market data				
S_0	r_d	r_f		
103.06	0.013	0.0319		

Table 3. Contract data for fader option pricing.

K	L	H	T	Fixing
EUR/AUD contract data				
1.6411	1.4770	1.8052	1.0082	Monthly
USD/JPY contract data				
103.06	92.7540	113.3660	1.0082	Monthly

Table 4. Numerical results for fader call option values in the Heston model.

	Scenario EUR/AUD	Scenario USD/JPY
Monte Carlo	0.0566	2.5594
0.975 confidence interval	(0.0566, 0.0567)	(2.5560, 2.5629)
Numerical Integration	0.0566	2.5563
Fast Fourier transform	0.0542	2.5588

Table 5. Contract data for discrete barrier option pricing.

Scenario	K	H	T
Down-and-out EUR/AUD	1.4770	1.5590	1.0082
Up-and-out USD/JPY	82.4480	123.6720	1.0082

parameter is negative and the speed of mean reversion is low.

In the following, the problem of pricing fader and discretely monitored barrier options is discussed on the basis of these two FX market data examples with regard to the computational accuracy between the previously described pricing methods.

5.3.2. Fader options. For the comparison of computational accuracy we price fade-in calls as stated in (23) with the two example sets of model parameters described in the previous section and the contract data of the option given in table 3. The fade-in levels were chosen as a fixed range $[S_0 - 10\% S_0,\ S_0 + 10\% S_0]$. The time to maturity of the option is set to approximately one year and a monthly fixing.

The computational results on the analysis of the accuracy of the different numerical methods to price V_{fader} are summarized in table 4. The analytic values are calculated with the numerical multidimensional integration functions provided by MatLab. The Monte Carlo simulations are performed by following the sampling scheme described in section 5.2 using one million spot paths. They use volatility values, which are observed from the volatility process at 100 points in time between each fixing during the lifetime of the option. Additionally, an antithetic variance reduction method is used. The parameters for the FFT are chosen as $N = 512$ integration grid points and $\Delta = 0.3$.

Since the value of the fader option given in (23) is equal to the sum of fadlets $V_F(t_i)$, for $i = 1, \ldots, 12$, divided by 12, the total accuracy is determined by the corresponding results of each summand. The outputs of all numerical methods mostly yield the same results up to at least the second decimal place. We note that, of the methods we examined, the FFT method is the fastest, but using a different numerical integration implementation than that within MatLab might be more suitable. This is followed up in the next section on the numerical results of discretely monitored barrier options.

5.3.3. Discrete barrier options. The analysis of the valuation of discretely monitored barrier options is initiated by a comparison of the available pricing methods with respect to computational accuracy. Again we work with the example settings in tables 1 and 2, and the contract data of the barrier options is specified in table 5. We use the following methods for the calculation of one value of a particular discrete barrier option.

- *Monte Carlo simulation with one million spot paths*. For the discretization of the time horizon of the volatility process, a Euler scheme as in section 5.2 and 100 steps between each fixing were chosen. This discretization of the variance process is fine enough for this example to ensure that the distribution of the logarithmic spot value at the first time step approximates the true value sufficiently well. An antithetic variance reduction method was applied.
- *Fast Fourier transform methods as described in the previous section*. The parameters of the FFT method were set to values between $N = 2^4$ and $N = 2^7$, and the discretization grid for the numerical integration was chosen equally for every dimension, i.e. $\Delta = 0.5$ in the down-and-out case and $\Delta = 0.3$ in the up-and-out case.
- *Multidimensional numerical integration*. The multidimensional integral is estimated using a Romberg integration method based on the midpoint rule. The number of subintervals into which the ith integration interval is initially subdivided is set to 30 for the case of up-and-out calls and to 60 for down-and-out calls. This integration technique was developed by

Table 6. Values for a discretely monitored down-and-out barrier option with parameters given in table 5 for three different numerical methods.

Number of fixings	Monte Carlo simulation (0.975 confidence)	Fast Fourier transform (N)	Multi-dimensional numerical integration (# subdivisions)
2	0.1966	0.1968	0.1967
	(0.1965, 0.1967)	(1024)	(60)
3	0.1911	0.1917	0.1911
	(0.1909, 0.1912)	(256)	(60)
4	0.1874	0.1576	0.1873
	(0.1873, 0.1875)	(64)	(30)
5	0.1846		0.1845
	(0.1844, 0.1847)		(15)
6	0.1824		0.1824
	(0.1822, 0.1826)		(15)

Table 7. Values for a discretely monitored up-and-out barrier option with parameters given in table 5 for three different numerical methods. We used $\alpha = 1.75$.

Number of fixings	Monte Carlo Simulation (0.975 confidence)	Fast Fourier transform (N)	Multi-dimensional numerical integration (# subdivisions)
2	18.9197	18.9227	18.9208
	(18.9064, 18.9338)	(1024)	(30)
3	18.9095	18.9631	18.9063
	(18.8962, 18.9229)	(256)	(30)
4	18.8946	17.4414	18.8956
	(18.8812, 18.9080)	(64)	(30)
5	18.8691		18.8694
	(18.8557, 18.8826)		(20)

Davis and Rabinowitz (1984). The C++ version of this integration method can be found at http://people.scs.fsu.edu/ burkardt/cpp_src/nintlib/nintlib.C.

We illustrate the values of discrete down-and-out barrier options with different numbers of fixings n, for $n = 1, \ldots, 6$,

$$(S_{t_n} - K)^+ \prod_{i=1}^{n} 1\!\!1_{\{S_{t_i} \geq H\}},$$

where the fixing times $t_i = \{1/n,\ 2/n, \ldots, 1\}$ are chosen equidistant from each other. The results using Monte Carlo simulation, numerical integration and FFT are listed in table 6. For the comparison of computational accuracy, the method of multidimensional numerical integration is applied with respect to formula (30).

We observe that the values for the down-and-out barrier options with fixings up to three lie close together for all three numerical methods. The values that are computed with FFT and the numerical integration lie in the 97.5% confidence intervals of the Monte Carlo simulations. The values of the Monte Carlo simulation with one million simulated spot paths and the values of the other two methods coincide up to the third decimal place for the EUR/AUD market scenario and up to the first decimal place for the USD/JPY market scenario, which is equivalent to an accuracy of one-tenth of a percent of the underlying. The same accuracy could not be achieved for barrier options with more than three fixings, which is a result of the small number of grid points N used in the FFT method. Note that we used the FFT routine of Numerical Recipes (Press *et al.*, 1993), which requires a one-dimensional input array of size $2 \cdot N^{\#\text{ fixings}}$. Due to memory capacity, this limits the number of grid points N for the case of five and six fixings to $N = 32$ and $N = 16$, respectively. Hence, N can only be increased if the FFT method is called multiple times for different integration regions. Consequently, by dividing the calls of the FFT routine into several single calls, the deviation of the values between Monte Carlo and FFT could be corrected. However, the multidimensional numerical integration routine is not limited to a certain number of grid points and therefore the values computed with this method result in a higher accuracy than the results obtained with FFT, but, as expected, it also requires much more computational time. Hence, we limited our analysis to discrete barriers with six fixings. The results of the multidimensional integration and the Monte Carlo simulation show an accuracy of 0.1% of the underlying for discrete barrier options with at least five or six fixings.

For the calculation of values of up-and-out barrier options with fixings n, for $n = 1, \ldots, 6$,

$$(S_{t_n} - K)^+ \prod_{i=1}^{n} \mathbb{1}_{\{S_{t_i} \leq H\}}, \quad \text{for } t_i = \left\{\frac{1}{n}, \frac{2}{n}, \ldots, 1\right\},$$

the technique of multidimensional numerical integration uses formula (29) and the result of corollary 4.1. Basically, the numerical integration uses the multivariate characteristic functions given in equation (6) and (15). The fast Fourier transform method depends on the same functions, but extended to complex arguments. Therefore, comparison of the two methods mainly lies in the comparison of the computational time. All the results for the three numerical methods are listed in table 7.

The computational time of the FFT routine for up-and-out barrier options is double that for the down-and-out case, since here the FFT routine has to be called twice, because of (35). However, for the multidimensional numerical integration routine the computational time is reduced, as the overall accuracy can already be achieved with half the number of initial subintervals used for the down-and-out barrier case.

In the one-dimensional case the computational time of the FFT routine to compute vanilla option values compared with numerical integration with certain caching techniques is longer, as reported by Kilin (2007). However, in the multivariate case, our examples show that the choice between the various numerical methods (without caching techniques) is not such a clear-cut decision.†

As a final comment we note that, clearly, a Monte Carlo simulation or solutions via the Heston partial differential equations are the preferred methods for pricing weakly path-dependent options with a dependence on the underlying spot of more than three points in time. However, our semi-analytical formulas can help with the benchmarking or even just testing the implementations of these methods. We can also envisage situations where closed-form formulas give a competitive edge over numerical methods. For a running contract, for example, we eventually get to a point with very few fixings left, which is close to expiry. For such a case we need a very precise and fast evaluation, which also allows the computation of Greeks. Our result could help there.

6. Summary

We have shown how to compute values of faders and discretely monitored barrier options in the Heston model in closed form by extending the valuation method using multiple Fourier transforms. The resulting characteristic function of a vector of logarithmic spot prices can be computed explicitly using a recursion. The methodology presented extends to other stochastic volatility models. The important property turns out to be a known characteristic function. We have also demonstrated that our results can be used in practical situations. We have benchmarked and verified our closed-form solutions in a multidimensional integration and an FFT method against Monte Carlo.

Acknowledgement

For their help and financial support we wish to express our thanks to Lucht Probst Associates GmbH.

References

Albecher, H., Mayer, P., Schoutens, W. and Tistaert, J., The little Heston trap. *Wilmott*, 2007, **1**, 83–92.

Andersen, L., Simple and efficient simulation of the Heston stochastic volatility model. *J. Comput. Finance*, 2008, **11**(3).

Becker, C. and Wystup, U., On the cost of delayed fixing announcements in FX options markets. *Ann. Finance*, 2009, **5**(2), 161–174.

Broadie, M. and Kaya, Ö., Exact simulation of stochastic volatility and other affine jump diffusion models. *Oper. Res.*, 2006, **54**(2), 217–231.

Carr, P. and Madan, D., Option valuation using the fast Fourier transform. *J. Comput. Finance*, 1999, **2**(4), 61–73.

Chiarella, C. and Ziogas, A., American call options under jump-diffusion processes – A Fourier transform approach. *Appl. Math. Finance*, 2009, **16**(1), 37–79.

da Fonseca, J., Grasselli, M. and Tebaldi, C., Wishart multi-dimensional stochastic volatili. Working Paper, 2005.

Davis, P. and Rabinowitz, P., *Methods of Numerical Integration*, 1984 (Dover: New York).

Dempster, M. and Hong, S., Spread option valuation and the fast Fourier transform, in *Proceedings of the International Conference on Computational Finance and its Applications*, 2000.

Duffie, D., Singleton, K. and Pan, J., Transform analysis and asset pricing for affine jump-diffusions. *Econometrica*, 2000, **68**, 1343–1376.

Faulhaber, O., Analytic methods for pricing double barrier options in the presence of stochastic volatility. Master's Thesis, 2002.

Grünbichler, A. and Longstaff, F., Valuing futures and options on volatility. *J. Bank. Finance*, 1996, **20**, 985–1001.

Hakala, J. and Wystup, U., *Foreign Exchange Risk*, 2002 (Risk Books: London).

Heston, S.L., A closed-form solution for options with stochastic volatility with applications to bond and currency options. *Rev. Financial Stud.*, 1993, **6**, 327–343.

Higham, D. and Mao, X., Convergence of Monte Carlo simulations involving the mean-reverting square root process. *J. Comput. Finance*, 2005, **8**(3), 35–62.

Kahl, C. and Lord, R., Complex logarithms in Heston-like models. *Math. Finance*, 2010, **20**(4), 671–694, forthcoming.

Kilin, F., Accelerating the calibration of stochastic volatility models. Research Report No. 6, Frankfurt School of

†Note that when evaluating options with different strike and barrier levels we do not need to recompute the characteristic function when evaluating the integrals in (30).

Finance & Management, Center for Practical Quantitative Finance, 2007.

Kluge, T., Pricing derivatives in stochastic volatility models using the finite difference method. Diploma Thesis, Technical University of Chemnitz, 2003.

Kruse, S. and Nögel, U., On the pricing of forward starting options in Hestons model on stochastic volatility. *Finance Stochast*., 2005, **9**, 233–250.

Lee, R.W., Option pricing by transform methods: Extensions, unification and error control. *J. Comput. Finance*, 2004, **7**(3), 51–86.

Lipton, A., *Mathematical Methods for Foreign Exchange*, 2001 (World Scientific: Singapore).

Lord, R., Condition and conquer – Pricing of baskets, Asians and swaptions in general models. *5th Winter School on Financial Mathematics*, 2006. Available online at: http://web.wits.ac.za/NR/rdonlyres/DA62AFD2-4DA5-451D-B4E1-44E50EA1D21B/0/RoelofMSc.pdf.

Lord, R., Koekkoek, R. and van Dijk, D., A comparison of biased simulation schemes for stochastic volatility models. *Quant. Finance*, 2010, **10**(2), 177–194.

Mikhailov, S. and Nögel, U., Heston's stochastic volatility model: Implementation, calibration and some extensions. *Wilmott Mag*., 2003, 74–79.

Overhaus, M., *et al*., *Modelling and Hedging Equity Derivatives*, 1999 (Risk Books: London).

Press, W.H., Flannery, B.P., Teukolsky, S.A. and Vetterling, W.T., *Numerical Recipes in C*, 1993 (Cambridge University Press: Cambridge).

Shephard, N.G., From characteristic function to distribution function: A simple framework for the theory. *Econ. Theory*, 1991, **7**(4), 519–529.

Wystup, U., *FX Options and Structured Products*, 2006 (Wiley: New York).

Zhu, J., *Modular Pricing of Options – An Application of Fourier Analysis*, 2000 (Springer: Berlin).